

Estimating Stochastic Gravitational Wave Backgrounds with Sagnac Calibration

Craig J. Hogan

Astronomy and Physics Departments, University of Washington, Seattle, Washington 98195-1580

Peter L. Bender

JILA, University of Colorado and National Institute of Standards and Technology, Boulder, Colorado 80309-0440

Armstrong *et al.* have recently presented new ways of combining signals to precisely cancel laser frequency noise in spaceborne interferometric gravitational wave detectors such as LISA [1–4]. One of these combinations, which we will call the “symmetrized Sagnac observable”, is much less sensitive to external signals at low frequencies than other combinations, and thus can be used to determine the instrumental noise level [4]. We note here that this calibration of the instrumental noise permits smoothed versions of the power spectral density of stochastic gravitational wave backgrounds to be determined with considerably higher accuracy than earlier estimates, at frequencies where one type of noise strongly dominates and is not substantially correlated between the six main signals generated by the antenna. We illustrate this technique by analyzing simple estimators of gravitational wave background power, and show that the instrumental sensitivity to broad-band backgrounds at some frequencies can be improved by a significant factor of as much as $(f\tau/2)^{1/2}$ in spectral density h_{rms}^2 over the standard method, where f denotes frequency and τ denotes integration time, comparable to that which would be achieved by cross-correlating two separate antennas. The applications of this approach to studies of astrophysical gravitational wave backgrounds generated after recombination and to searches for a possible primordial background are discussed. With appropriate mission design, this technique allows an estimate of the cosmological background from extragalactic white dwarf binaries and will enable LISA to reach the astrophysical confusion noise of compact binaries from about 0.1 mHz to about 20mHz. In a smaller-baseline follow-on mission, the technique allows several orders of magnitude improvement in sensitivity to primordial backgrounds up to about 1 Hz.

I. INTRODUCTION

In ground-based interferometric gravitational wave detectors such as LIGO, VIRGO, GEO-600 and TAMA, stochastic backgrounds will be best detected by correlating signals from more than one interferometer within a wavelength of each other. If in-common noise sources can be eliminated, the correlation allows a direct estimate of the “noise” coming from gravitational waves, separately from instrumental sources of noise. In this way the detection of a broad-band background can take advantage of a broad detection bandwidth B , and sensitivity to rms strain in a broad band grows with time like $h_{rms} \propto (B\tau)^{-1/4}$.

The problem is different for the Laser Interferometer Space Antenna (LISA) [5], which consists of three spacecraft in a triangle configuration. Although two “independent” observables can be measured with this arrangement, yielding orthogonal polarization information for sources, the observable signals are not truly independent since they include correlated instrumental noise. Separation of the instrumental noise from stochastic gravitational wave signals requires an alternative approach, as well as careful attention to correlations in the different types of noise affecting the signals.

A fundamental recent development has been the introduction by Armstrong *et al.* of a new way of precisely cancelling laser frequency noise in interferometric gravitational wave detectors where the arm lengths are not exactly equal [1–3]. It is shown in these papers that for a triangular geometry as is used in LISA, the signals from detectors in the different satellites can be combined, if the hardware allows, to give various observables that are free of the laser frequency noise. In addition, several of these observables have considerably reduced sensitivities to gravitational wave signals at low frequencies (below about 30 mHz, corresponding to the 33-second roundtrip light travel time on one arm of the triangle). The observables α, β and γ defined in [1] correspond to Sagnac observables: they correspond to taking the difference in phase for laser beams that have gone around the triangle in opposite directions, each starting from a different spacecraft.

However, another of the observables defined in [1], called ζ , has even less sensitivity to gravitational waves at low frequencies. We will refer to it as the “symmetrized Sagnac observable”, since the signals that are combined to form ζ are the same as for α, β and γ , but they are evaluated at very nearly the same time instead of at substantially different times. This observable allows a more complete “switching off” of the sky signal, and can be used to give a valuable determination of the other sources of noise in the interferometer, as discussed in [1–3].

More recently, Tinto *et al.* [4] have discussed the problem of separating the confusion noise due to many unresolvable galactic and extragalactic binaries in each frequency bin from instrumental noise. In particular, they consider the

case where the confusion noise level is comparable with or larger than the instrumental noise level. They show that what we are calling the symmetrized Sagnac observable permits the confusion noise level to be established reliably.

What apparently has not been pointed out previously is that using the symmetrized Sagnac observable to calibrate the instrumental noise potentially makes possible considerably higher sensitivity for determining smoothed values of the power spectral density for broad-band isotropic gravitational wave backgrounds, such as binary confusion backgrounds or primordial stochastic backgrounds. For each frequency bin, with a width roughly equal to the inverse of the data record length, the noise power in the sky signal can be separated from the instrumental noise power by using estimators which combine the symmetrized Sagnac observable with the other observables (such as Michelson observables) which are fully sensitive to gravitational waves. For isotropic backgrounds with fairly smooth spectra, the precision can be improved substantially by integrating the estimated power spectral density over many spectral bins, after removing and fitting out recognizable binary sources. In this paper we discuss this idea and its impact on studies of backgrounds observable by LISA and by a possible high-frequency follow-on mission. Our main conclusion is that this capability should be included in science optimization studies for the detailed mission design for LISA.

II. ESTIMATING STOCHASTIC BACKGROUNDS USING THE SYMMETRIZED SAGNAC OBSERVABLE AND A BROAD BANDWIDTH

For simplicity, we will consider only the 6 Doppler signals y_{ij} ($i, j = 1, 2, 3$) introduced by Armstrong et al. in [1], rather than the more complete results including the additional 6 signals z_{ij} given by Estabrook et al. [3] to allow for having two separate proof masses in each spacecraft. This corresponds to setting the z_{ij} in [3] equal to zero. The two lasers in each spacecraft are thus assumed to be perfectly phase locked together, but to run independently of the lasers in the other two spacecraft. On each spacecraft, the phases of the beat signals between the laser beams from the two distant spacecraft and the local lasers are measured as a function of time and recorded. This gives the total of 6 signals that are considered. They are sent to a common spacecraft and then combined, with time delays equal to the travel times over different sides of the triangle, to give various different observables that are free of the phase noise in the lasers.

The data combinations relevant for this discussion are illustrated in Figure 1. Although laser and optical bench noise exactly cancel in these combinations, they contain various mixtures of gravitational wave signals and instrumental noise. The Sagnac observables α , β and γ have a lower sensitivity for gravitational waves at frequencies near 1 mHz than do the Michelson observables X , Y , Z discussed by Armstrong et al. Thus, we will base our strategy on using the observables X , Y and Z to detect the gravitational waves, and the symmetrized Sagnac observable ζ to calibrate the noise.

The technique usually considered for estimating the stochastic background is to use time variations in the observed power during the year to model out noise sources with non-isotropic components such as confusion noise from galactic binaries. (Integration over a year will give a nearly isotropic response to incoming gravitational wave power [6–8].) However, the uncertainty in the instrumental noise level still remains. The sensitivity is then limited to a factor of order unity times that obtainable in one frequency resolution element, $\delta f \approx \tau^{-1}$, where τ is the length of the time series. This factor is the fractional uncertainty in the level of the instrumental noise. In effect this means that the sensitivity to stochastic backgrounds does not increase with time. The technique we propose is to use ζ to calibrate the noise power levels differentially in each frequency bin, i. e. use Sagnac calibration, allowing a sum of sky signal from a broad bandwidth, $B \approx f/2$. For broadband backgrounds, this approach begins to “win” after an integration time $\tau \approx 2f^{-1}$.

We now sketch in more detail a specific strategy for analysing the data. This strategy allows an accurate calibration of the main sources of noise entering into the y_{ij} , without assuming that these either are the same or are known a priori. We adopt the notation of [3], and assume that the complex Fourier coefficients X_k , Y_k , Z_k and ζ_k for X , Y , Z and ζ have been derived from a long data set, such as perhaps a year of observations. We also define η_k^2 as the mean of the squares of the absolute values of X_k , Y_k , and Z_k .

Since the laser noise C_{ij} exactly cancels for these combinations, the main instrumental noise sources are due to the noninertial changes in the velocities of the proof masses \vec{v}_{ij} (the “proof mass noise” $y_{ij}^{proof\ mass}$) and the combination of noise from pointing errors, shot noise, and other optical path effects (the “optical path noise” $y_{ij}^{optical\ path}$). From eqs. 3.5 and 3.6 in [3], and from cyclic perturbations of eqs. 3.1 and 3.2, with the $z_{ij} = 0$, the noise power spectral densities $S_X(f)$, $S_Y(f)$, $S_Z(f)$ and $S_\zeta(f)$, without gravitational waves, can be obtained in terms of the $y_{ij}^{proof\ mass}$ and $y_{ij}^{optical\ path}$. We define $S_{ave}(f)$ to be the average of $S_X(f)$, $S_Y(f)$ and $S_Z(f)$, and $\langle S_y^{proof\ mass} \rangle$ and $\langle S_y^{optical\ path} \rangle$ to be the averages of the corresponding noise power spectral densities for the 6 signals y_{ij} . Then we obtain the same

results as for eqs. 4.1 and 4.3 in [3], except with $S_X(f)$ replaced by $S_{ave}(f)$ and with $S_y^{proof\ mass}$ and $S_y^{optical\ path}$ replaced with their average values:

$$S_{ave}(f) = [16 \sin^2(2\pi fL)] \{ [2 \cos^2(2\pi fL) + 2] \langle S_y^{proof\ mass} \rangle + \langle S_y^{optical\ path} \rangle \} \quad (1)$$

$$S_\zeta(f) = 24 \sin^2(\pi fL) \langle S_y^{proof\ mass} \rangle + 6 \langle S_y^{optical\ path} \rangle. \quad (2)$$

These formulas do not assume that the noise contributions to the individual y_{ij} are the same.

The quantities X_k , Y_k , etc., can be divided into an instrumental noise part and a gravitational wave background part: i.e. $X_k = X_{n,k} + X_{GW,k}$, etc. We can then define an estimator E_k for the gravitational wave power,

$$E_k = \eta_k^2 - D(f) |\zeta_k|^2, \quad (3)$$

where

$$\eta_k^2 \equiv (1/3) [|X_k|^2 + |Y_k|^2 + |Z_k|^2]. \quad (4)$$

The coefficient $D(f)$ is defined in such a way that the noise component of the second term subtracts (on average) the noise component of the first, leaving only contributions from the gravitational wave power of both terms; that is, $\langle E_k \rangle$ is a known multiple of the GWB. In general $D(f)$ will be computed numerically based on a model of LISA and its noise sources. Here we estimate the bias in the estimate and the sensitivity level for a detection or upper limit based on E_k , for two situations where we can identify analytical approximations to $D(f)$ based on the simple model described above.

We first define a high-frequency estimator E_k for the GW background power, useful when the optical path noise dominates (but when f is not so high that the Sagnac combination becomes nearly fully sensitive to gravitational waves):

$$E_k = \eta_k^2 - [S_{ave}/S_\zeta]_{est} |\zeta_k|^2, \quad (5)$$

For frequencies high enough so that

$$R = \langle S_y^{proofmass} \rangle / \langle S_y^{opticalpath} \rangle \quad (6)$$

is small,

$$[S_{ave}/S_\zeta]_{est} = G_1(f) [(8/3) \sin^2(2\pi fL)], \quad (7)$$

where

$$G_1(f) = \frac{1 + 2[1 + \cos^2(2\pi fL)] R_{est}}{1 + 4[\sin^2(\pi fL)] R_{est}}. \quad (8)$$

To first order in the actual value of R minus the estimated value R_{est} , the bias in E_k is given by

$$(\delta E_k)_{bias} = [S_{ave}(f)] [2 + 2 \cos^2(2\pi fL) - 4 \sin^2(\pi fL)] [R - R_{est}]. \quad (9)$$

To the extent that the bias in E_k can be neglected, $\langle E_k \rangle$ depends just on the GWB power:

$$\langle E_k \rangle = S_{GW,ave} - [(8/3) \sin^2(2\pi fL)] S_{GW,\zeta} \quad (10)$$

where $S_{GW,ave}$ is defined as

$$S_{GW,ave} = \langle \eta_{GW,k}^2 \rangle \quad (11)$$

and

$$S_{GW,\zeta} = \langle |\zeta_{GW,k}|^2 \rangle = \epsilon S_{GW,ave}. \quad (12)$$

At frequencies which are not too high, the Sagnac gravitational wave sensitivity is low so $\epsilon \ll 1$. The estimator is most useful at frequencies low enough so that $\langle E_k \rangle$ is comparable with $S_{GW,ave}$ and thus can be used to estimate the

GW background power efficiently. For LISA with triangle sides of length $L = 5 \times 10^6$ km, or 16.67 seconds in units with $c = 1$, this condition is satisfied if $f \leq f_{crit} \approx 25$ mHz.

The sensitivity to GWB is given by estimating the uncertainty δE_k in $\langle E_k \rangle$ from the relation

$$\delta E^2 = \langle E_k^2 \rangle - \langle E_k \rangle^2. \quad (13)$$

This is done in the appendix. The results are found to depend on the individual noise spectral densities for the six main LISA signals, rather than just their average value. For the case of all six noise spectral densities being equal, the results are:

$$\delta E^2 \approx [(64/3) \sin^4(\omega L)][9 + 4 \cos(\omega L) - \cos(2\omega L)] \langle S_y^{opticalpath} \rangle^2, \quad (14)$$

$$\delta E \leq [16 \sin^2(\omega L)] S_y^{opticalpath}. \quad (15)$$

If we let $\delta E = \lambda \langle \eta_{n,k}^2 \rangle$, then the factor λ characterizes the noise level of the estimate relative to an ideal instrument-noise-limited measurement.

Similarly, for very low frequencies where $R \gg 1$ and the proof mass noise dominates, the estimator becomes

$$E_k = \eta_k^2 - G_2(f)[(16/3) \cos^2(\pi f L)][1 + \cos^2(2\pi f L)]|\zeta|^2 \quad (16)$$

where

$$G_2(f) = \frac{1 + R_{est}^{-1}[2 + 2 \cos^2(2\pi f L)]^{-1}}{1 + R_{est}^{-1}[4 \sin^2(\pi f L)]^{-1}}. \quad (17)$$

In this case, for all six noise spectral densities equal, δE_k can be shown to be

$$\delta E_k \approx [(2/3) + (4/3) \cos(\omega L) + (5/6) \cos^2(\omega L)]^{1/2} \langle S_y^{proofmass} \rangle. \quad (18)$$

The interesting frequency range with $R \gg 1$ is near 100 microhertz, and thus ωL is very small, giving

$$\lambda \approx (17/6)^{1/2} = 1.7. \quad (19)$$

It should be noted that, for frequencies $f \lesssim 100$ microhertz, the combination $[(R_{est})^{-1}]/4 \sin^2(\omega L/2)$ in the denominator of Equation (17) is expected to be small for LISA even though (ωL) is very small. Thus $G_2(f)$ will be very close to unity, and the bias in $E_{k,n}$ is negligible.

The standard estimate of the amplitude signal-to-noise ratio S/N for detecting a gravitational wave background is given by

$$(S/N)_k^2 = \frac{S_{GW,X}}{\langle |X_{n,k}|^2 \rangle}. \quad (20)$$

As noted above, this sensitivity estimate implicitly assumes that the uncertainty in estimating the instrumental noise power level is about the same as the level itself. However, the error in estimating the instrumental noise level may well be highly correlated over a bandwidth comparable with the frequency, so that averaging the results from many frequency bins gains little if anything.

With the symmetrized Sagnac calibration approach, the S/N contributions from individual frequency bins are given by

$$(S/N)_k^2 = \{1 - [(8/3) \sin^2(\omega L)]\epsilon\} \frac{S_{GW,ave}}{\lambda \langle \eta_{n,k}^2 \rangle}. \quad (21)$$

Thus there are two possible inefficiency factors, characterized by ϵ and λ . However, these are more than offset for detecting broad-band backgrounds, since the contributions from individual frequency bins can now be averaged over a bandwidth of roughly $f/2$ to give an improvement in $(S/N)^2$ by a factor of about $(f\tau/2)^{1/2}$. Since $S_{GW,ave} = S_{GW,X}$ for an isotropic background, the overall reduction in the rms background gravitational wave amplitude needed in order to achieve $S/N = 1$ can be as large as a factor

$$F = \{1 - [(8/3) \sin^2(\omega L)]\epsilon\}^{1/2} \left[\frac{f\tau}{2\lambda^2} \right]^{1/4}, \quad (22)$$

relative to the standard estimated sensitivity. The symmetrized Sagnac calibration approach achieves about the same gain in sensitivity as the cross-correlation approach employed by ground-based experiments, and discussed by Ungarelli and Vecchio [9] for two separate LISA-type space-based antennas.

The discussion above has implicitly assumed that the dominant instrumental noise contributions to all of the six recorded signals y_{ij} are not correlated in phase. This is certainly true for the shot noise, but careful instrumental design will be necessary to make it a useful approximation for other noise sources. For example, wobble of the pointing of a given spacecraft could give rise to correlated noise in the received signals at the other two spacecraft due to wavefront distortion. Also, correlated proof mass acceleration noise for two proof masses on the same spacecraft can occur if the effect of common temperature variations is significant. A quantitative discussion of such correlations will be required before the extent of realistically feasible improvements in stochastic background measurements can be determined. However, this is beyond the scope of our current knowledge of such effects. We therefore will assume that the six signals may have different noise levels but are uncorrelated in phase. Our results thus are rough upper limits to the possible improvements with the symmetrized Sagnac calibration method.

III. SENSITIVITY LIMITS AND BINARY BACKGROUNDS

The approximate threshold sensitivity of the planned LISA antenna with 5×10^6 km arm lengths and for a signal-to-noise ratio $S/N = 1$ is shown in Figure 2. The sensitivity using the standard Michelson observable can be approximated by a set of power law segments:

$$\begin{aligned} h_{rms} &= 1.0 \times 10^{-20} [f/10mHz]/\sqrt{Hz}, & 10mHz < f \\ &1.0 \times 10^{-20}/\sqrt{Hz}, & 2.8mHz < f < 10mHz \\ &7.8 \times 10^{-18} [(0.1mHz/f)^2]/\sqrt{Hz}, & 0.1mHz < f < 2.8mHz \\ &7.8 \times 10^{-18} [(0.1mHz/f)^{2.5}]/\sqrt{Hz}, & 0.01mHz < f < 0.1mHz \end{aligned} \quad (23)$$

where the sensitivity has been averaged over the source directions. Below 100 μ Hz there is no adopted mission sensitivity requirement, but the listed sensitivity has been recommended as a goal for frequencies down to at least 10 μ Hz, provided that the cost impact is not too high.

A number of authors have discussed the expected levels of gravitational wave signals due to binaries in our galaxy, and the essentially isotropic integrated background from all other galaxies out to large red shifts. The normalization is uncertain, since only a few binaries above 0.1 mHz in frequency are known, since they were selected from highly biased surveys, and since the evolutionary history for some is poorly constrained. We adopt most of the levels estimated in [10] for the total binary backgrounds, with estimates from [11] for the reduction of confusion noise at higher frequencies by fitting out Galactic binaries. The estimate for helium cataclysmics discussed in [12] is not included.

For close white dwarf binaries (CWDBs), a factor of 10 lower space density than the maximum yield estimated earlier from models of stellar populations (e.g. [13]) is assumed. However, the resulting value is within a factor 2 of the latest theoretical estimate of Webbink and Han [14]. The factor 10 reduction factor is conventional, as discussed near the end of [10], and gives a signal level a factor $10^{1/2}$ lower than given in Table 7 of [10]. It should be noted that there is about a factor of three uncertainty in the estimated total galactic signal level, and the estimated extragalactic signal level is even more uncertain. The ratio of extragalactic to galactic signal amplitudes is taken to be 0.2 for CWDBs and 0.3 for neutron star (NS) binaries. (A ratio of 0.3 was found by Kosenko and Postnov [15] for CWDBs with an assumed history of the star formation rate and for cosmological parameters $\Omega_{tot} = 1$ and $\Omega_{\Lambda} = 0.7$. However, the value of 5.5 kpc that they used for the scale height of the distribution perpendicular to the plane of the disk is more appropriate for neutron stars, and a reduction by a factor of about 1.5 is needed for a CWDB scale height near 90 pc.)

Below about 1 mHz there are so many galactic binaries that there will be many per frequency bin for one year of observations, and only a few of the closest ones can be resolved. Above roughly 3 mHz most Galactic binaries will be a few frequency bins apart, and can be solved for despite sidebands due to the motion and orientation changes of the antenna. The effective spectral amplitude of the confusion noise from both galactic and extragalactic binaries remaining after the resolved binaries have been fitted out of the data record (see e.g. [11]) is shown in Figure 2. Essentially none of the extragalactic stellar-mass binaries can be resolved with LISA's sensitivity (in contrast to intense signals from an expected small number involving massive black holes (MBHs)).

Except for the shot noise, it is difficult to know what the instrumental noise level is to better than perhaps a factor of two by conventional methods. Tinto et al. [4] have emphasized the value of using the symmetrized Sagnac calibration to determine the total gravitational wave signal for frequencies of roughly 200 μHz to 3 mHz, where the expected level is above that of the optical path measurement noise. Our main point is that, after using Sagnac calibration in properly selected frequency bands where either the optical path noise or the proof mass noise dominates strongly, averaging over a bandwidth comparable with the frequency considerably reduces the instrument noise in measurements of the smoothed spectral amplitude. This allows better sensitivity for measurement of stochastic backgrounds over a larger range of frequencies.

The possible improvement factor above 5 mHz is up to about $(f\tau/2)^{1/4}$, which equals 20 at 10 mHz, but two types of limitations have to be considered also. One is due to the uncertainty in R_{est} at 10 mHz and below. The other is due to the similar gravitational wave sensitivities of η and ζ at frequencies of 25 mHz and above. We estimate that the resulting overall sensitivity improvement factor for LISA would be between 10 and 20 for frequencies of about 10 to 25 mHz.

At frequencies below 200 μHz , the improvement factor is about $(f\tau/6)^{1/4}$. At 100 μHz this is a factor of about 5, so the sum of the galactic and extragalactic backgrounds could be determined down to somewhat lower frequencies than otherwise would be possible.

IV. SAGNAC CALIBRATION WITH ENHANCED HIGH-FREQUENCY LISA FOLLOW-ON MISSION

If the LISA mission indeed finds several types of sources involving massive black holes, there will be strong scientific arguments for follow-on missions aimed at achieving considerably higher sensitivity at both lower and higher frequencies. Some preliminary discussion of possible follow-on missions has been given by Folkner and Phinney [16] and Ungarelli and Vecchio [9]. In order to give some indication of the future background accuracy achievable by calibrating and smoothing, we consider an illustrative example of a high frequency follow-on mission.

We assume the same basic triangular geometry and 60 degree ecliptic inclination as for LISA, but the arm lengths are 50,000 km instead of 5×10^6 km. The noise level for the gravitational sensors (i.e. free mass sensors) is a factor of ten lower than for LISA, and the fractional uncertainty in measuring changes in the distances between the test masses is 30 times lower than for LISA. It should be remembered that making the arm lengths much shorter also makes the the requirements on the laser beam pointing stability and on the fraction of a fringe to which phase measurements have to be made much tighter. The shorter antenna might have the rates of change of the distances between the test masses kept constant to make the phase measurements on the signals easier, provided that the required forces on the test masses can be kept free enough of noise.

The extragalactic CWDB background would be gone above about 0.1 Hz, provided that merger-phase and ringdown radiation from coalescences are not significant. At higher frequencies, the binary background is expected to be almost entirely due to extragalactic neutron star binaries and 5 or 10 solar mass black hole binaries. We take the neutron star binary coalescence rate in our galaxy to be $1 \times 10^{-5} \text{yr}^{-1}$, which is a factor of 10 lower than assumed in table 7 of [10]. This estimate may still be somewhat on the high side and has a high uncertainty [17], but we regard it as giving a plausible estimate of the total gravitational wave background level, allowing for some additional contribution from black hole binaries. We also increase the expected gravitational wave amplitude by a factor 1.5 to allow very roughly for eccentricity of the NS-NS binaries [18]. With the ratio of 0.3 between the extragalactic and galactic amplitudes from [15], this gives an extragalactic amplitude of $h_{rms,XGNSB} = 8 \times 10^{-25} f^{-7/6} \text{Hz}^{-1/2}$. The background sensitivity with the Sagnac calibration gets within a factor of 4 of this extragalactic NS plus BH binary background at 0.5 Hz. The follow-on antenna would give detailed measurements of the gravitational wave background spectrum up to about 100 mHz, as well as limits at higher frequencies and much improved measurements of coalescences of binaries at cosmological distances containing intermediate mass black holes.

V. INFORMATION CONCERNING EXTRAGALACTIC ASTROPHYSICAL BACKGROUNDS

For the LISA mission, the Sagnac calibration approach will make possible measurements of the extragalactic CWDB background (XGCWDB) at frequencies from about 5 to 25 mHz. This is important because it will give new information on the star formation rate at early times. Kosenko and Postnov [15] have investigated the effect of a peak in the star formation rate at redshifts of $z = 2$ or 3 on XGCWDB, with emphasis on the observed frequency range from 1 to 10 mHz. However, going to somewhat higher frequency would improve the sensitivity to the star formation rate.

The CWDBs [10–15,19–21] include He-He, He-CO and CO-CO white dwarf binaries, as well as a few binaries containing the rarer O/Ne/Mg white dwarfs. Here He and CO stand for helium and carbon/oxygen white dwarfs respectively. Rough estimates of the comparative rms signal strengths for the first three types as a function of frequency are given in Fig. 1 of [11]. It can be seen that the frequency cutoffs due to coalescence are different for the different types, ranging roughly from 15 mHz for the first type to 60 for the third. This is mainly because the He dwarfs are less massive and larger than the CO dwarfs. In addition, the total binary mass ranges for the three types, in units of the solar mass, are about 0.50-0.75, 0.75-1.45 and 1.45-2.4, which means that there is a range of coalescence frequencies for each type.

The He-He binaries will contribute the most to determining the star formation rate, since their coalescence frequencies at redshifts of 2 or 3 will shift down into the accurately observable 10 to 25 mHz frequency range and thus will change the way in which the XGCWDB varies with frequency. Information on the distribution of chirp masses for the different types of CWDBs in our galaxy can be obtained from the resolved signals above about 3 mHz. However, careful studies will be needed in order to determine the sensitivity of the resulting star formation history to factors such as possible differences in the CWDB chirp mass distribution at earlier times.

The possible high-frequency LISA follow-on mission with Sagnac calibration would give an upper limit to the combined extragalactic NS-NS, NS-BH and BH-BH binary backgrounds between 0.1 and 1 Hz. For the CO-CO binaries, the highest frequency signals will come from the merger phase of coalescence and from possible ringdown of the resulting object, if two conditions are met: that the orbit is nearly circular before coalescence, and that a supernova not result. Even though all redshifts will be integrated over, the shape of the upper end of the CWDB background seems likely to still give new information on the binary mass distribution, the coalescence process and the star formation history.

Above 0.1 or 0.2 Hz but below the range of ground-based detectors, no other astrophysical backgrounds have been suggested except those due to extragalactic NS-NS, NS-BH and BH-BH binaries. Only a crude estimate for the combined background level has been included in this paper, and it is highly uncertain. As has been suggested by a number of authors, the BH-BH binaries may be the dominant source (see e.g. [22,17]). Higher levels would permit LISA follow-on observations up to somewhat higher frequencies, where possible confusion with a high frequency tail from CO-CO white dwarf merger phase or post-merger ringdown would be reduced. Approximate information on the relative strengths of the NS and BH binary backgrounds probably will be available from ground-based observations of the coalescence rates, but probably with only the BH-BH coalescences going out to substantial redshifts. Thus the main new information from LISA follow-on observations of these backgrounds may be on the history of the NS binary formation rates.

VI. PRIMORDIAL BACKGROUNDS

We have been characterizing backgrounds by h_{rms}^2 , the spectral density of the gravitational wave strain (also sometimes denoted S_h). For cosmology, we are interested in sensitivity in terms of the broadband energy density of an isotropic, unpolarized, stationary background, whose cosmological importance is characterized by

$$\Omega_{GW}(f) \equiv \rho_c^{-1} \frac{d\rho_{GW}}{d\ln f} = \frac{4\pi^2}{3H_0^2} f^3 h_{rms}^2(f) \quad (24)$$

where we adopt units of the critical density ρ_c . The broadband energy density per e -folding of frequency, $\Omega_{GW}(f)$, is thus related to the rms strain spectral density by [23]

$$\frac{h_0^2 \Omega_{GW}}{10^{-8}} \approx \left(\frac{h_{rms}(f)}{2.82 \times 10^{-18} \text{ Hz}^{-1/2}} \right)^2 \left(\frac{f}{1 \text{ mHz}} \right)^3, \quad (25)$$

where h_0 conventionally denotes Hubble's constant in units of $100 \text{ km s}^{-1} \text{ Mpc}^{-1}$. In these units, the main sources of instrumental and astrophysical noise are summarized schematically in Figure 3.

Primordial backgrounds can be produced by a variety of classical mechanisms producing relativistic macroscopic or mesoscopic energy flows at $T \geq 100 \text{ GeV}$, whose only observable relic is a gravitational wave background [23–25]. Because the gravitational radiation processes are not perfectly efficient, the total energy density $\int d\ln f \Omega_{GW}$ in gravitational waves must be less than that in the thermal relativistic relic particles (photons and three massless neutrinos) where the “waste heat” resides today, $\Omega_{rel} h_0^2 = 4.17 \times 10^{-5} T_{2.728}^4$, where h_0 refers to the Hubble constant. (The integrated density is already limited by nucleosynthesis arguments to less than about 0.1 of this value because

of the effect on the expansion rate.) It is interesting to pursue stochastic backgrounds as far as possible below this maximal level since most predicted effects, for example waves from even strongly first-order phase transitions, are at least several orders of magnitude weaker.

The spectrum of the background conveys information on early stages of cosmic history. Classical processes typically produce backgrounds with covering a broad band around a characteristic frequency determined by the scale of the energy flows, fixed by the gravitational timescale. The band accessible to the proposed space interferometers, 10^{-5} to 1 Hz, corresponds to the redshifted Hubble frequency from cosmic temperatures between about 100 GeV and 10^4 TeV—often thought to include processes such as baryogenesis and supersymmetry breaking, and possibly also activity in new extra dimensions [26,27]. We adopt the point of view that it is interesting to explore new regions of frequency and amplitude for broad-band backgrounds, regardless of theoretical justifications for a particular scale. We present in Figure 4 a summary of the likely accessible parameters (frequency and amplitude) for primordial backgrounds, optimistically taking account of the improvements suggested here, both for LISA and the illustrative high-frequency successor considered earlier.

A much more ambitious goal often cited is detection of gravitational waves expected from the quantum fluctuations of the graviton field during inflation. These occur at all frequencies up to the redshifted Hubble frequency from the inflationary epoch (which may exceed 10^{12} Hz), but are in general much weaker than the classical sources; a naïve estimate is that $\Omega_{GW,inflation} \approx h_{inflation}^2 \Omega_{rel}$ where $h_{inflation} \approx (H_{inflation}/M_{Planck})$ is the amplitude of tensor metric quantum fluctuations on the Hubble scale, and $H_{inflation}$ is the Hubble constant during inflation. From the microwave background anisotropy we estimate that on large scales, $h_{inflation} \approx (\delta T/T)_{tensor} \leq 10^{-5}$. Unless the spectrum is “tilted” in an unexpected direction (larger $H_{inflation}$ on smaller scales, which inflate last), this is an upper limit on the quantum effects and is a rough estimate of where gravitational wave data set limits on “generic” models of inflation. The corresponding $h_0^2 \Omega_{GW} \approx 10^{-15}$ is about ten orders of magnitude below the maximal classical level, and well below the astrophysical binary noise.

The problem of separating primordial backgrounds from binary backgrounds depends to some extent on how different the spectra are. From general scaling arguments [26], classical phase transitions, where the radiation is emitted over a short period of time, tend to generate spectra with a steep low frequency limit, scaling like $\Omega_{GW} \propto f^7$ to f^6 . The high frequency limit in some models (involving defects such as light cosmic strings or Goldstone waves, or brane displacement modes) may be scale-invariant, $\Omega_{GW} \propto \text{constant}$; in phase transitions it falls off at least as fast as $\Omega_{GW} \propto f^{-1}$ and can be even steeper. Even though these processes have characteristic frequencies, the primordial spectrum is quite broad and is not expected to have sharp features that would stand out as diagnostics. At frequencies above 100 mHz, where the astrophysical confusion background is mainly from neutron star and black hole binaries (for which the main energy loss is gravitational radiation), it obeys the scaling $\Omega_{GW} \propto f^{2/3}$. At lower frequencies the dominant XGCWDB spectrum departs from this due to redshift and various nongravitational effects on the binary population, as discussed earlier; in the 10 to 100 mHz range the dominant XGCWDBs are predicted to closely mimic a scale-free spectrum. Depending on the situation, spectral features may or may not clearly distinguish a primordial component.

For the LISA mission with Sagnac calibration, the estimated astrophysical background apparently can be detected with $S/N \approx 10$ from 10 to 25 mHz, but because of the uncertainties in modeling XGCWDB, it is not clear whether a primordial contribution could be detected for a level much less than $h_0^2 \Omega_{GW} \approx 10^{-10}$. On the other hand, the range of frequencies over which the primordial background search can be carried out at this level is substantial, especially if we include the possible LISA follow-on mission discussed earlier (see Figure 4). With the high-frequency antenna, the results with Sagnac calibration may reach a level below $h_0^2 \Omega_{GW} \approx 10^{-11}$ at a frequency above 0.1 Hz where there is a drop in the astrophysical backgrounds.

VII. APPENDIX: δE FOR HIGH-FREQUENCY ESTIMATOR

The uncertainty δE in estimating $\langle E_k \rangle$ can be estimated from the relation

$$\delta E^2 = \langle E_k^2 \rangle - \langle E_k \rangle^2. \quad (26)$$

We will be dealing with E_k , but drop the subscript k for now. Expanding Eq. (5) into noise and wave parts,

$$\begin{aligned} 3E = & \{[|X_n|^2 + |Y_n|^2 + |Z_n|^2] - [8 \sin^2(2\pi fL)]|\zeta_n|^2\}_1 \\ & + \{[(X_n)(X_{GW})^* + (Y_n)(Y_{GW})^* + (Z_n)(Z_{GW})^*] - [8 \sin^2(2\pi fL)(\zeta_n)(\zeta_{GW})^*] + c.c.\}_2 \\ & + \{[|X_{GW}|^2 + |Y_{GW}|^2 + |Z_{GW}|^2] - [8 \sin^2(2\pi fL)]|\zeta_{GW}|^2\}_3 \end{aligned} \quad (27)$$

For frequencies where $S_{GW,ave}$ is small compared with $S_{n,ave}$ and where $|\zeta_{GW}|^2$ can be neglected,

$$E \approx (1/3)\{\}_{1} + (1/3)[|X_{GW}|^2 + |Y_{GW}|^2 + |Z_{GW}|^2]; \quad (28)$$

since the noise terms average to zero,

$$\langle E \rangle \approx S_{GW}, \quad (29)$$

(as promised for the estimator, by design), and since their spectral density dominates the GW terms,

$$\langle E^2 \rangle \approx (1/9)\langle [\{\}_{1}]^2 \rangle. \quad (30)$$

We assume that the lengths of the three arms for LISA are nearly equal to their average value L . From the definitions of X, Y, Z and ζ in ref. [3]:

$$X = (y_{32} - y_{23})[e^{3i\omega L} - e^{i\omega L}] + (y_{31} - y_{21})[e^{2i\omega L} - 1], \quad (31)$$

$$Y = (y_{13} - y_{31})[e^{3i\omega L} - e^{i\omega L}] + (y_{12} - y_{32})[e^{2i\omega L} - 1], \quad (32)$$

$$Z = (y_{21} - y_{12})[e^{3i\omega L} - e^{i\omega L}] + (y_{23} - y_{13})[e^{2i\omega L} - 1], \quad (33)$$

$$\zeta = [(y_{32} + y_{21} + y_{13}) - (y_{23} + y_{31} + y_{12})]e^{i\omega L}. \quad (34)$$

Then:

$$|X|^2 = 4 \sin^2(\omega L)[|y_{32} - y_{23}|^2 + |y_{31} - y_{21}|^2 + \{(y_{32} - y_{23})(y_{31}^* - y_{21}^*)e^{i\omega L} + c.c.\}], \quad (35)$$

etc. From such expressions, it can be shown that:

$$\langle E^2 \rangle \approx (32/9) \sin^4(\omega L) \{ \langle \Xi_1 \rangle + [5 + 4 \cos(\omega L)] \langle \Xi_2 \rangle + [6 - 2 \cos(2\omega L)] \langle \Xi_3 \rangle \}, \quad (36)$$

where

$$\Xi_1 = |y_{32}|^2 |y_{23}|^2 + |y_{21}|^2 |y_{12}|^2 + |y_{13}|^2 |y_{31}|^2 + |y_{31}|^2 |y_{21}|^2 + |y_{12}|^2 |y_{32}|^2 + |y_{23}|^2 |y_{13}|^2, \quad (37)$$

$$\Xi_2 = |y_{23}|^2 |y_{31}|^2 + |y_{31}|^2 |y_{12}|^2 + |y_{12}|^2 |y_{23}|^2 + |y_{32}|^2 |y_{13}|^2 + |y_{13}|^2 |y_{21}|^2 + |y_{21}|^2 |y_{32}|^2, \quad (38)$$

$$\Xi_3 = |y_{32}|^2 |y_{31}|^2 + |y_{13}|^2 |y_{12}|^2 + |y_{21}|^2 |y_{23}|^2. \quad (39)$$

It is clear from these expressions that the uncertainty δE in E depends on the instrumental noise levels in the six main signals, rather than just on their average. Assuming, however, that they are all equal and uncorrelated gives the following estimates:

$$\langle E^2 \rangle = (64/3) \sin^4(\omega L) [9 + 4 \cos(\omega L) - \cos(2\omega L)] \langle S_y^{opticalpath} \rangle^2, \quad (40)$$

$$\delta E < 16 \sin^2(\omega L) \langle S_y^{opticalpath} \rangle. \quad (41)$$

In general, even if the instrumental noise levels are unequal, it can be shown that δE is less than $\sqrt{9/8}\eta^2$, so that $\lambda \lesssim \sqrt{9/8} \approx 1$ for frequencies from 5 to 25 mHz.

ACKNOWLEDGMENTS

It is a pleasure to thank John Armstrong, Frank Estabrook and Massimo Tinto for extensive discussions of their laser phase noise correction method and particularly for emphasizing the possibility of using the Sagnac observable to correct for instrumental noise. We also thank the following for valuable discussions of what could be achieved by possible LISA follow-on missions: Sterl Phinney, Bill Folkner, Ron Hellings, Bernard Schutz, Carlo Ungarelli, Alberto Vecchio, Karsten Danzmann, and Neil Christianson. This work was supported at the University of Washington by NSF and at the University of Colorado by NASA.

-
- [1] J. W. Armstrong, F. B. Estabrook, & M. Tinto, ApJ 527, 814 (1999)
 - [2] M. Tinto & J. Armstrong, Phys. Rev. D 59, 102003 (1999)
 - [3] F. B. Estabrook, M. Tinto & J. W. Armstrong, Phys. Rev. D 62, 042002 (2000)
 - [4] M. Tinto, J. W. Armstrong & F. B. Estabrook, Phys. Rev. D, 63, 021101 (R) (2000)
 - [5] K. Danzmann, in “Laser Interferometer Space Antenna: Proc. 2nd Int. LISA Symp.”, Amer. Inst. Phys. Conf. Proc. Vol. 456, ed. W. M. Folkner, p. 3 (1998); W. M. Folkner, loc. cit., p. 11; R. T. Stebbins, loc. cit., p. 17; B. F. Schutz, Class. Quant. Grav. 16, A131 (1999); P. L. Bender, in “Gravitational Waves”, eds. I. Ciufolini, V. Gorini, V. Moschella, and P. Fre, (Inst. of Phys. Publishing, Bristol, UK), (2001)
 - [6] G. Giampieri, MNRAS 289, 185 (1997)
 - [7] G. Giampieri, & A. G. Polnarev, MNRAS 291, 149 (1997)
 - [8] G. Giampieri & A. G. Polnarev, Class. Quant. Grav. 14, 1521 (1997)
 - [9] C. Ungarelli & A. Vecchio, Phys. Rev. D. 63, 064030 (2001)
 - [10] D. Hils, P. L. Bender, & R. F. Webbink, ApJ 360, 75 (1990)
 - [11] P. L. Bender & D. Hils, Class. Quant. Grav. 14, 1439 (1997)
 - [12] D. Hils & P. L. Bender, ApJ 53, 334 (2000)
 - [13] R. F. Webbink, Astrophys. J. 277, 355 (1984)
 - [14] R. F. Webbink & Z. Han, in “Laser Interferometer Space Antenna: Proc. 2nd Int. LISA Symp.”, loc. cit., p. 61 (1998)
 - [15] D. I. Kosenko & K. A. Postnov, Astron. Astrophys. 336, 786 (1998)
 - [16] W. M. Folkner & E. S. Phinney, private communication (1999)
 - [17] V. Kalogera, in *Gravitational Waves: Third Edoardo Amaldi Conference*, ed. S. Meshkov (AIP Conf. Proc. Vol. CP523), 41 (2000)
 - [18] D. Hils, Astrophys. J. 381, 484 (1991)
 - [19] G. Nelemans, S. F. Portegies Zwart, & F. Verbunt, astro-ph/9903255 (2000)
 - [20] R. Schneider, V. Ferrari, S. Matarrese & S. F. Portegies Zwart, Mon. Not. R. Astron. Soc., submitted, astro-ph/0002055 (2000)
 - [21] G. Nelemans, F. Verbunt, L. R. Yungelson & S. F. Portegies Zwart, Astron. Astrophys., 360, 1011 (2000)
 - [22] B. F. Schutz, Class. Quant. Grav. 16, A131 (1999)
 - [23] M. Maggiore, Phys. Rep. 331, 283 (2000)
 - [24] A. Kosowsky, A. Mack, & T. Kahniashvili, “Stochastic Gravitational Radiation from Phase Transitions”, to appear in proceedings of Astrophysical Sources of Gravitational Radiation for Ground-Based Detectors, Drexel University, Oct. 30 - Nov. 1 (2000), astro-ph/0102169
 - [25] R. Apreda, M. Maggiore, A. Nicolis, & A. Riotto “Supersymmetric Phase Transitions and Gravitational Waves at LISA,” hep-ph/0102140
 - [26] C. J. Hogan, Phys. Rev. Lett. 85, 2044 (2000)
 - [27] C. J. Hogan, Phys. Rev. D 62, 121302 (2000)

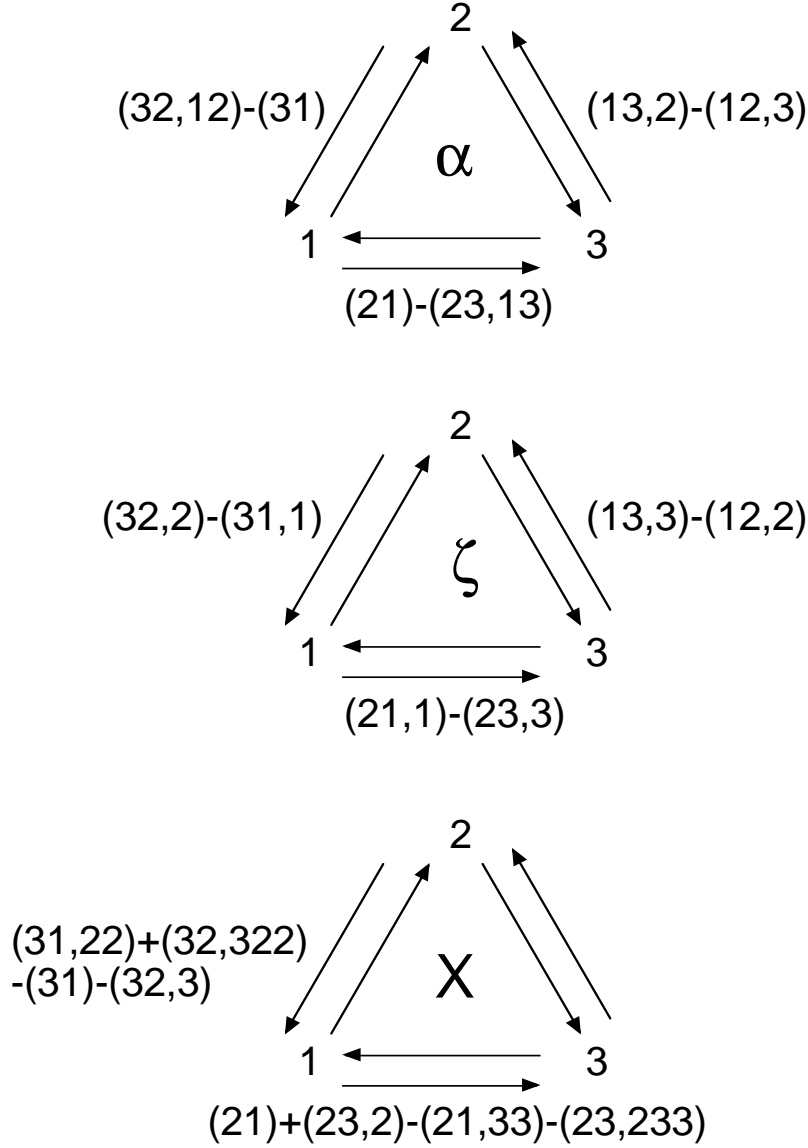


FIG. 1. Illustration of the signal combinations discussed in the text. The numbers labelling each pair of arrows correspond to the subscript labels of signals in the notation of Armstrong et al.: “12,3” for example refers to $y_{12,3}$, the signal traveling on the side opposite spacecraft 1, received by spacecraft 2 (from spacecraft 3), with a time delay corresponding to the light travel time along the side opposite 3. The β and γ observables correspond to cyclic permutations of the indices for α . The symmetrized Sagnac observable ζ is very similar to the round-trip-difference observables α, β, γ , except that for ζ all the signals are compared with almost the same time delays, leading to a minimal sensitivity to low-frequency gravitational waves. The X observable is based on a Michelson interferometer using only two sides, but is the difference in signals at two times separated by approximately the the round trip travel time on one arm. The Y and Z observables are equivalent to X but based on the other spacecraft pairings.

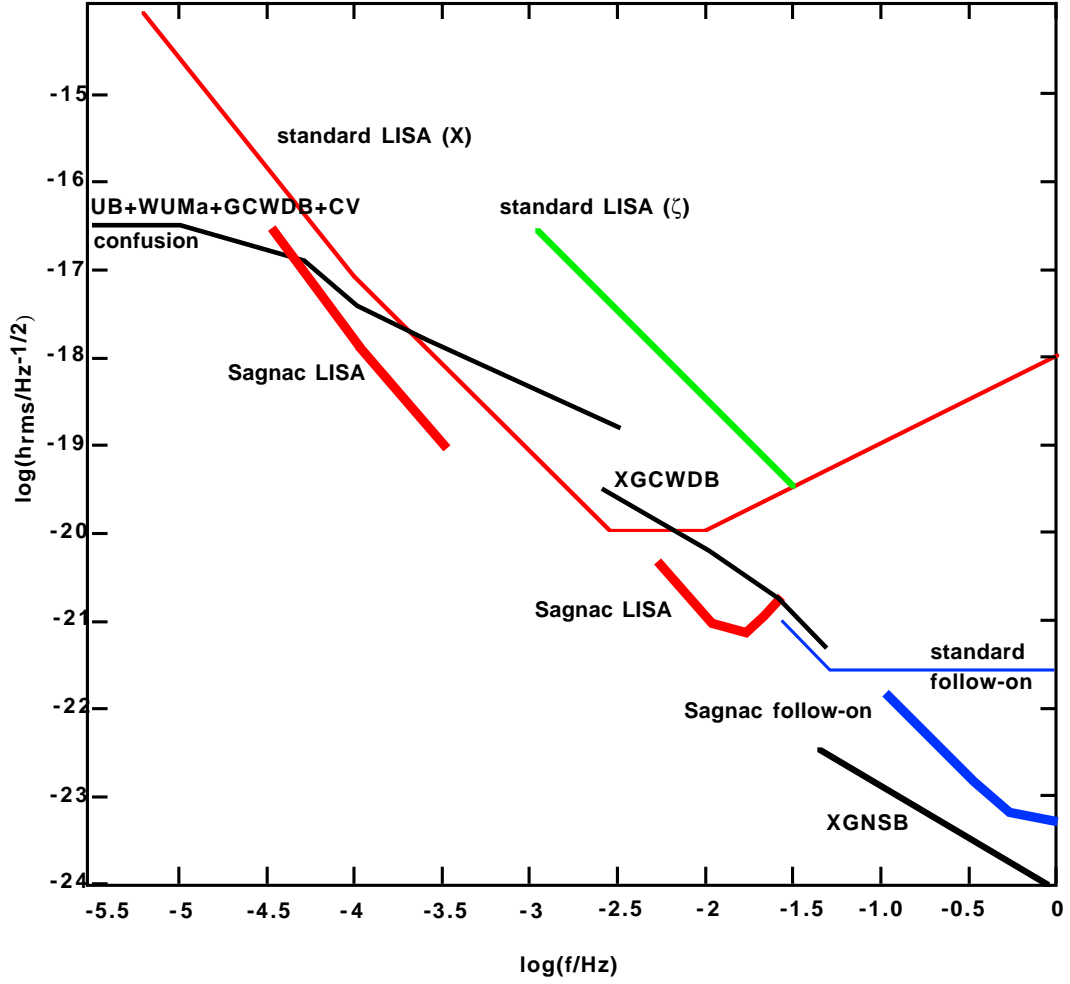


FIG. 2. Instrument sensitivity in terms of rms strain per $\sqrt{\text{Hz}}$, to broad band backgrounds, assuming a one year integration. The “standard” S/N=1 levels in one frequency resolution element, for LISA and for the shorter-baseline follow-on mission described in the text, are shown as lighter lines. The sensitivity is shown for both the (standard) Michelson observable X and the symmetrized Sagnac observable ζ . The levels theoretically attainable with Sagnac calibration and averaging over bandwidth $f/2$ are shown in bold lines. The Sagnac estimator loses its advantage at high frequencies where ζ is no longer insensitive to gravitational waves; the analytic form for the estimator discussed here is also inefficient at frequencies where the proof mass noise and optical path noise are comparable. At low frequencies where proof mass noise dominates, another analytic form yields a significant improvement in sensitivity, which allows the confusion background to be measured to lower frequencies. Estimated astrophysical backgrounds are shown for Galactic binaries, extragalactic white dwarf binaries, and extragalactic neutron star or black hole binaries.

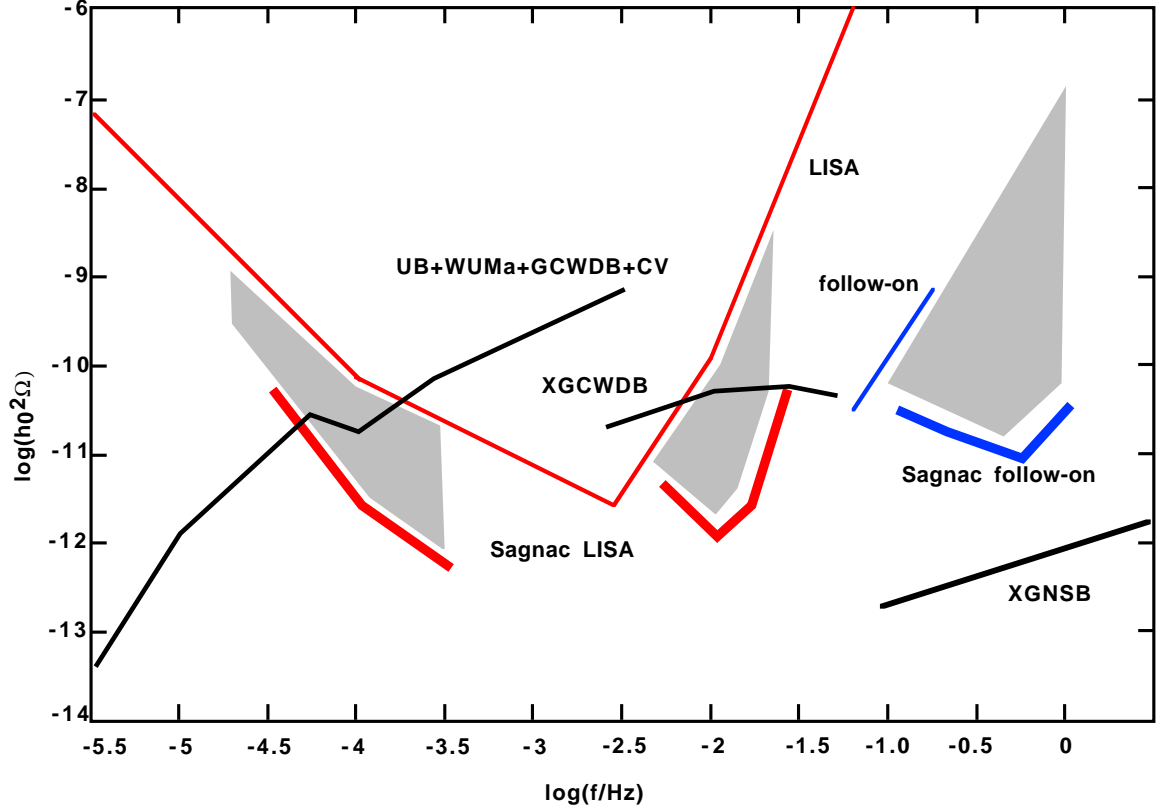


FIG. 3. Noise levels are shown in terms of the equivalent energy density of an isotropic stochastic background. Units are the energy density per factor e of frequency, in units of the critical density, normalized for Hubble constant $h_0 = 1$. Where applicable, a one-year integration is assumed. The sum UB+WUMa+GCWDB represents the estimated confused background from the sum of unevolved Galactic binaries, W Ursa Majoris binaries and white dwarf binaries. These estimates are uncertain by about a factor of 10 in Ω . The confusion noise level drops abruptly above the frequency where almost all Galactic binaries can be fitted out. Extragalactic white-dwarf binaries “XGCWDB” create a stochastic confusion noise which cannot be eliminated. At still higher frequencies above about 0.1 Hz, the white dwarfs coalesce, leaving only the confusion background from extragalactic neutron star binaries and stellar-mass black hole binaries (XGNSB). The LISA instrument noise limit ($S/N=1$) after one year is shown, both the traditional narrow-band sensitivity and the broad-band sensitivity allowed by Sagnac calibration and discussed here. The shaded regions show the main areas for improvement possible from using Sagnac calibration. The Sagnac technique allows a significantly improved measurement of a low resolution spectrum of the confusion background with LISA both at low frequencies $\approx 0.1\text{mHz}$ and at higher frequencies to $\geq 20\text{ mHz}$, including an accurate measurement with LISA of the extragalactic white dwarf binary confusion background. The Sagnac sensitivity limit for the smaller-baseline follow-on mission is shown for the parameters discussed in the text; in this case the Sagnac technique offers a more substantial overall improvement in sensitivity.

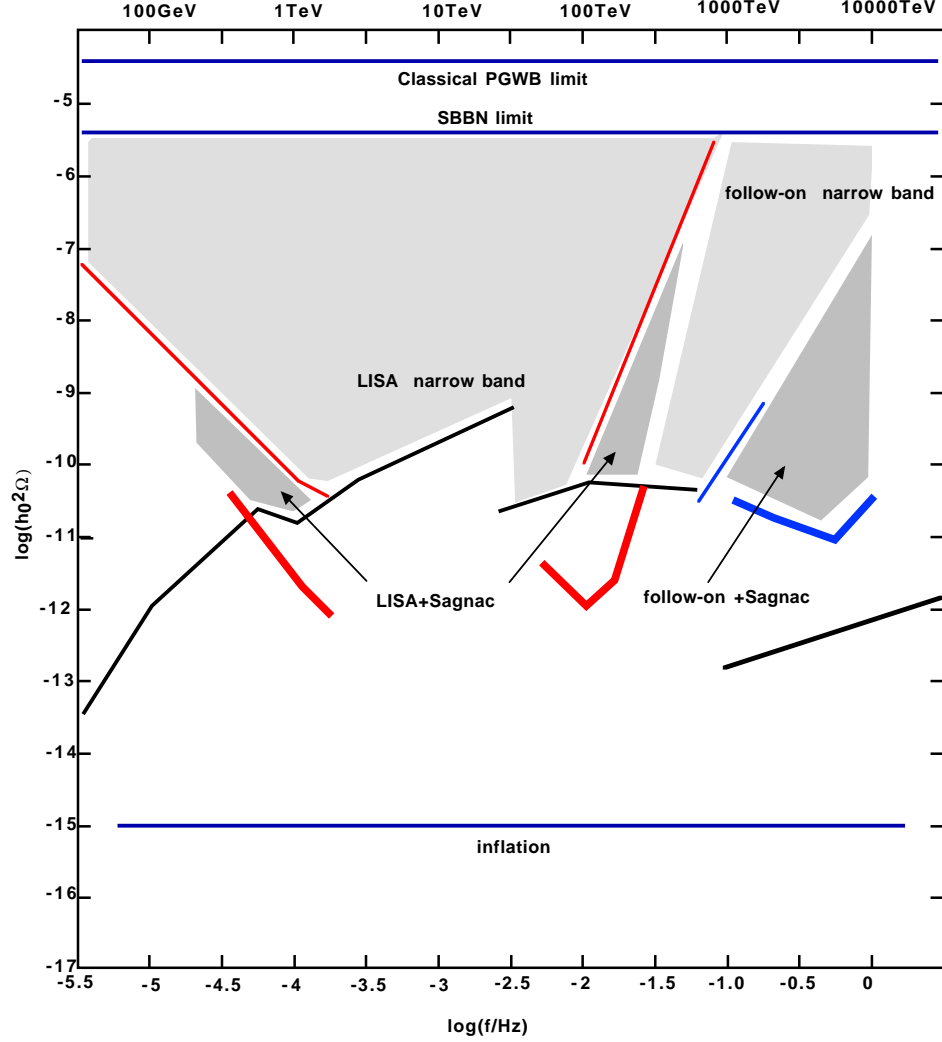


FIG. 4. Regions of new parameter space for primordial backgrounds opened up by proposed experimental setups and data analysis strategies. Scale on the top axis shows the cosmic temperature for which classical waves generated at the Hubble frequency and redshifted to the present yield the observed frequency on the bottom axis. Several characteristic energy densities are shown: Classical primordial gravitational wave background limit (PGWB) shows the sum of energies of photons and massless neutrinos, the maximal level expected for primordial backgrounds; “SBBN” denotes the maximum level consistent with Standard Big Bang Nucleosynthesis (both of these for a background with $\Delta f = f$); and “inflation” denotes a typical, untilted, scale-free inflation-generated spectrum, at the maximum level consistent with the background radiation anisotropy. Shaded regions lie above both instrument noise and binary confusion backgrounds, where primordial backgrounds can be detected. The darker-shaded regions show the extra benefit (for primordial background measurements) of Sagnac calibration with both missions.